

Comparison of the toxicity of sintered and unsintered indium-tin oxide particles in murine macrophage and epidermal cells

Nicole S. Olgun ^{a,*}, Anna M. Morris ^a, Tabatha Lynn Barber ^a, Aleksandr B. Stefaniak ^b, Michael L. Kashon ^a, Diane Schwegler-Berry ^a, Kristin J. Cummings ^b, Stephen S. Leonard ^a

^a Health Effects Laboratory Division, National Institute for Occupational Safety and Health, Morgantown, WV, USA

^b Respiratory Health Division, National Institute for Occupational Safety and Health, Morgantown, WV, USA

ARTICLE INFO

Article history:

Received 28 January 2017

Revised 19 May 2017

Accepted 24 May 2017

Available online xxxx

Keywords:

Indium

Metals

Occupational health

Sintering

ABSTRACT

Indium-tin oxide (ITO) is used to produce flat panel displays and several other technology products. Composed of 90% indium oxide (In_2O_3) and 10% tin oxide (SnO_2) by weight, ITO is synthesized under conditions of high heat via a process known as sintering. Indium lung disease, a recently recognized occupational illness, is characterized by pulmonary alveolar proteinosis, fibrosis, and emphysema. Murine macrophage (RAW 264.7) and epidermal (JB6) cells stably transfected with AP-1 to study tumor promoting potential, were used to differentiate between the toxicological profiles of sintered ITO (SITO) and unsintered mixture (UITO). We hypothesized that sintering would play a key role in free radical generation and cytotoxicity. Exposure of cells to both UITO and SITO caused a time and dose dependent decrease of the viability of cells. Intracellular ROS generation was inversely related to the dose of both UITO and SITO, a direct reflection of the decreased number of viable RAW 264.7 and JB6/AP-1 cells observed at higher concentrations. Electron spin resonance showed significantly increased hydroxyl radical ($\cdot OH$) generation in cells exposed to UITO compared to SITO. This is different from LDH release, which showed that SITO caused significantly increased damage to the cell membrane compared to UITO. Lastly, the JB6/AP-1 cell line did not show activation of the AP-1 pathway. Our results highlight both the differences in the mechanisms of cytotoxicity and the consistent adverse effects associated with UITO and SITO exposure.

© 2017 Published by Elsevier Inc.

1. Introduction

Indium-tin oxide (ITO) thin films are widely used in the electronics industry for the production of transparent electrodes for liquid crystal display screens, along with flat panel displays, alkaline batteries, and various other technological applications. With unique properties such as high electrical conductivity and transparency, ITO is in high demand. Composed of 90% indium oxide (In_2O_3) and 10% tin oxide (SnO_2) by weight, ITO is synthesized under conditions of high heat via a process known as sintering. During this process, loose metal powders are bonded together first through local bonding between adjacent particles, followed by a later stage of pore-rounding and shrinking, ultimately transforming into solids at temperatures below their melting point (Hoganas, 2013; Lison et al., 2009).

With the increase in ITO demand and production in recent years, indium lung disease has been recognized amongst exposed workers (Nakano et al., 2016; Nakano et al., 2015). In 2003, the first case of indium-associated pulmonary toxicity was reported in Japan, one of the

world's largest manufacturers of ITO. The individual was diagnosed with interstitial pneumonia, where histopathological analysis of the lung biopsy revealed alveolar spaces filled with red blood cells, fibrin, cholesterol clefts, alveolar macrophages, and numerous fine particles, consistent with ITO particle inhalation (Homma et al., 2003). Amongst workers with indium lung disease, other reported clinical features include cough, fibrosis, abnormal pulmonary function tests, pulmonary alveolar proteinosis (PAP), and emphysematous changes (Nakano et al., 2016; Cummings et al., 2012).

In cultured murine macrophage (RAW 264.7) and human bronchial epithelial cells (BEAS-2B), indium compounds have been shown to induce a pro-inflammatory response via activation of the nucleotide oligomerization domain-like receptor protein 3 inflammasome (NLRP3), which has been implicated in the development of pulmonary fibrosis (Badding et al., 2015; Biswas et al., 2011). In addition, rats exposed to SITO have exhibited pulmonary alveolar proteinosis with the presence of indium in the blood plasma used as a marker of exposure (Badding et al., 2016). Various studies have also suggested that the observed toxicities associated with indium compounds, can in part be attributed to their ability to generate reactive oxygen species (ROS). Indium is capable of interacting with hydrogen peroxide (H_2O_2) via Fenton-like reactions to produce $\cdot OH$, with the downstream effects being nucleic acid

* Corresponding author at: National Institute for Occupational Safety and Health, 1095 Willowdale Road, MS 2015, Morgantown, WV 26505, USA.

E-mail address: nolgun@cdc.gov (N.S. Olgun).

damage, lipid peroxidation and activation of programmed cell death pathways (Lison et al., 2009; Leonard et al., 2004; Jomova and Valko, 2011; Badding et al., 2014).

Previous work done by Leonard et al. has utilized ITO which had been in contact with metalworking fluid (MWF). It is not unusual for MWF, often used to reduce heat and friction and to remove metal particles in machining and grinding operations, to be contaminated with gram negative bacteria (Badding et al., 2016, 2014). Work-related asthma, hypersensitivity pneumonitis, chronic bronchitis and impaired lung function have all been associated with occupational exposure to MWF (Gilbert et al., 2010).

The ITO collected and used in the current work has never been in contact with MWF. Though the main goal of this study was to ascertain the differences between UITO and SITO in cells, we were also interested in whether or not contact with MWF played a role in the toxicities associated with ITO previously observed in murine macrophage RAW 264.7 cells, in which the ITO was baked to de-activate the endotoxin (Badding et al., 2016). The murine epidermal JB6 cell line, stably transfected with the AP-1 luciferase plasmid, was used to study the tumor promoting potential of ITO, since only limited evidence exists about its carcinogenic properties (Nagano et al., 2011).

In addition, though inhalation exposure to ITO is the primary cause for concern in relation to the development of pulmonary alveolar proteinosis, the potential toxicities associated with dermal exposure still need to be investigated. The Centers for Disease Control estimates that >13 million workers in the United States are occupationally exposed to >82,000 chemicals that can be absorbed through the skin (U.S.G.A.O, 2005). Studies done in mice have shown that topical exposure to UITO does in fact cause immune stimulation and has the potential to penetrate both intact and breached skin (Brock et al., 2014). With occupational exposure to indium on the rise (Tolcin, 2016; Hines et al., 2013), a better understanding ITO toxicity is needed to allow for improved worker health and safety.

2. Materials and methods

2.1. Indium collection

The indium used in this study was collected from a United States ITO production facility from production processes (NIOSH, 2012). In contrast to both SITO and UITO particles used in previous studies in our lab, ITO particles in this study were never exposed to MWF.

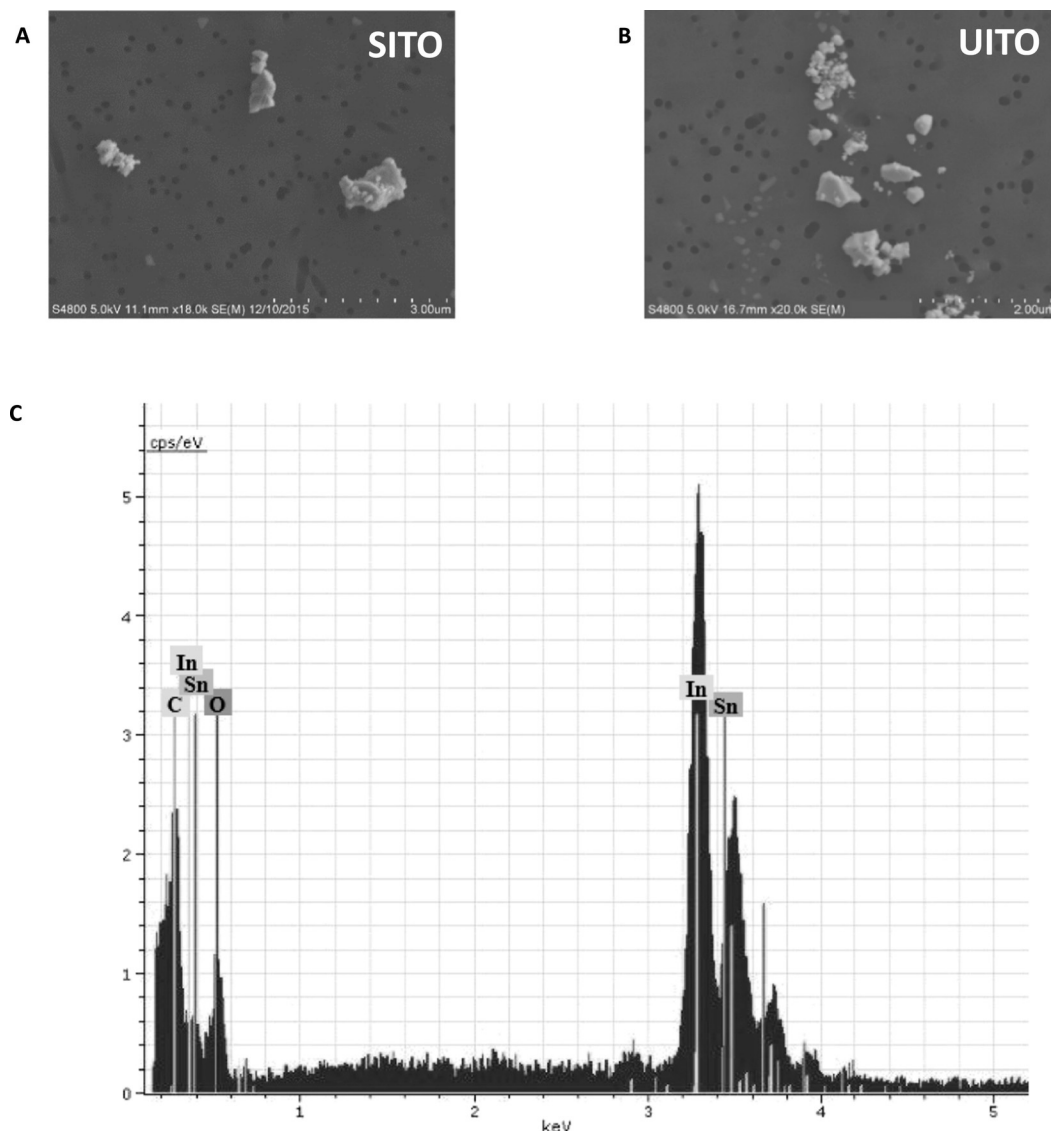


Fig. 1. Electron Microscopy and Elemental Analysis of SITO and UITO. Images obtained from field emission scanning electron microscopy (FE-SEM) confirm that both SITO (A) and UITO (B) particles were <5 μm in diameter. Images were acquired using 20,000× magnification using a 5.0 kV accelerating voltage. (C) Representative elemental analysis for both SITO (pictured) and UITO particles confirm the presence of indium, tin, carbon and oxygen.

2.2. Particle characterization

The morphology and size of ITO particles were determined using field emission scanning electron microscopy (FE-SEM). A 0.1% (w/w) suspension of particles using deionized water was prepared and sonicated for 3 min (energy delivered = 1000 J). The final concentration was 0.02% (w/w) and 1 ml was passed through a 0.1 μm polycarbonate filter (Steriltech Corp., Kent, WA). A section from each filter was imaged at 10 K magnification using 5 kV accelerating voltage (Hitachi S-4800, Hitachi High Technologies America, Inc., Dallas, TX). For elemental analysis, particles were analyzed by a Bruker EDX (Berlin, Germany), with the spectrum indicating the presence of indium and tin. Characteristics such as density, surface area, surface chemistry, and zeta potential have been previously determined and are not impacted by the presence or absence of MWF (Badding et al., 2014).

2.3. Cell culture

Murine macrophage (RAW 264.7) cells and murine epidermal cells (JB6) stably transfected with the AP-1 luciferase reporter plasmid were used for all experiments. RAW 264.7 cells were obtained from ATCC (Manassas, VA) while the JB6/AP-1 line was graciously donated by the laboratory of Dr. Min Ding (NIOSH, Morgantown, WV).

RAW 264.7 cells were cultured in Dulbecco's modified Eagle's medium (DMEM) supplemented with 10% fetal bovine serum (FBS) and 50 mg/ml of penicillin/streptomycin (Invitrogen Life Sciences, Grand Island, NY). Cells were maintained at 37 °C in a 5% CO₂ incubator and passaged by scraping into either medium or PBS, depending on the experiment. RAW 264.7 cells were chosen based on previous experiments where they have been shown to interact with ITO and also to study the effects of SITO and UITO on cells in the absence of endotoxin (Badding et al., 2014; Gwinn et al., 2013).

JB6 cells, stably transfected with the AP-1 luciferase reporter plasmid by the Ding lab, were cultured in Eagles minimum essential medium (EMEM) supplemented with 5% FBS, 50 mg/ml of penicillin/streptomycin and 2 mM L-glutamine (Sigma Aldrich, St. Louis, MO). Cells were maintained at 37 °C in a 5% CO₂ incubator and passaged using 0.01% trypsin (Gibco). This cell line was chosen to study the tumor promotion potential of ITO particles, since induction of the transcription factor AP-1 is associated with tumor promotion and progression (Kang et al., 2009; Ruocco et al., 2007).

2.4. Electron spin resonance

Electron spin resonance (ESR) trapping with 5'5-dimethylpyrroline N-oxide (DMPO) was used to detect the presence of short-lived free radical intermediates. The ability of ITO particles to produce •OH in cultured cells under Fenton-like reaction conditions with exposure to hydrogen peroxide (H₂O₂) was determined using a quartz flat cell assembly and Brüker EMX spectrometer (Billerica, MA).

For acellular ESR, a final concentration of 10 mg/ml ITO particles, 1 mM H₂O₂ and 100 mM DMPO was used. For cellular ESR, RAW 264.7 and JB6/AP-1 cells were used at a final concentration of 1 \times 10⁶ cells/ml, along with 10 mg/ml ITO particles, and 200 mM DMPO which were mixed with PBS and incubated at 37 °C for 5 min before being loaded into the flat cell for analysis. Peak heights were representative of relative levels of spin trapped •OH radicals.

2.5. Cell viability

The MultiTox-Fluor Multiplex Cytotoxicity Assay Kit from Promega (Madison, WI) was used for cell viability assays according to the manufacturer's instructions. RAW 264.7 cells (5 \times 10⁴/well) and JB6/AP-1 cells (4 \times 10⁴/well) were grown to ~80% confluence in 96-well plates. Cells were exposed to either 50 $\mu\text{g}/\text{ml}$, 150 $\mu\text{g}/\text{ml}$ or 250 $\mu\text{g}/\text{ml}$ of ITO particles or 1 mM Cr (VI) as a positive control for 4 h or 24 h.

The fluorogenic, cell permeant peptide substrate glycyl-phenylalanyl-aminofluorocoumarin (GF-AFC) was used to determine viability.

The dose of 50 $\mu\text{g}/\text{ml}$ has previously been calculated to represent approximately 3 years of average workplace exposure, whereas a higher dose of 1 mg/ml is more representative of a career-long exposure. The following formula was used based on airborne particle concentrations of 0.1 mg/m³ at the average resting human inhaled air volume over an 8 h workday, counting 260 workdays per year:

$$\text{Lung burden} = \text{respirable dust concentration} \times \text{inhaled air volume}/\text{workday} \times \text{alveolar deposition fraction} \times \text{days}.$$

The work done in this study therefore represents a range of exposures calculated to be at a minimum of 3 years, but less than a career long exposure (30–65 years, depending on the department within the indium plant) (Badding et al., 2014).

2.6. Lactate dehydrogenase (LDH) assay

The CytoTox96 Non-Radioactive Cytotoxicity Assay from Promega was used to quantitatively measure LDH release in cells according to the manufacturer's instructions. RAW 264.7 (5 \times 10⁴ cells/well) and JB6/AP-1 (4 \times 10⁴ cells/well) cells were plated in 96 well plates and exposed to either 50 $\mu\text{g}/\text{ml}$, 150 $\mu\text{g}/\text{ml}$ or 250 $\mu\text{g}/\text{ml}$ of ITO particles for 4 h or 24 h. The conversion of tetrazolium salt to formazan was used to measure the presence of LDH in culture media. An LDH positive control was included in the kit.

2.7. Comet assay

RAW 264.7 cells were grown to ~50% confluence and exposed to either 50 $\mu\text{g}/\text{ml}$, 150 $\mu\text{g}/\text{ml}$, or 250 $\mu\text{g}/\text{ml}$ of UITO, SITO, or 1 mM Cr (VI) as a positive control for 3 h and 24 h. Cells were then washed, scraped, and added to preheated agarose glass slides. Using an alkaline unwinding solution, cells were then lysed and subjected to electrophoresis at 21 V and 50 mA for 1 h (Trevigen, Inc., Gaithersburg, MD), causing any fragmented DNA to migrate out of the nuclear region of cells. Cells were then fixed with 70% ethanol overnight and labeled with SYBR green dye, which binds double stranded DNA. Images were acquired using an Olympus AX70 microscope with an Olympus DP73 digital camera (Olympus, Center Valley, PA). The Comet Assay IV software (Perceptive Instruments, Bury Saint Edmonds, United Kingdom) was used to count comet tails ($n = 50$ tails counted per experimental condition).

2.8. Intracellular reactive oxygen species (ROS) assay

RAW 264.7 (5 \times 10⁴ cells/well) and JB6/AP-1 (4 \times 10⁴ cells/well) cells were plated in 96 well plates and incubated with 2',7'-dichlorofluorescein diacetate (DCFH-DA), a cell permeable fluoroprobe, at a final concentration of 1 mM in serum-free DMEM for 45 min at 37 °C. Cells were washed two times in 1 \times PBS and DMEM was subsequently added back into the wells along with 50 $\mu\text{g}/\text{ml}$, 150 $\mu\text{g}/\text{ml}$ or 250 $\mu\text{g}/\text{ml}$ of ITO particles or 1 mM Cr(VI) as a positive control. Cells were then incubated for 2 h, 4 h, 6 h and 8 h at 37 °C. Plates were read at 485 nm excitation/530 nm emission at the end of respective timepoints to measure changes in fluorescence, which would be indicative of ROS production. For negative controls, DMEM and ITO particles were plated in wells in the absence of DCFH-DA and subtracted from the respective wells with exposed cells to account for any auto fluorescence.

2.9. Luciferase assay

To determine the tumor promotion potential of ITO particles in the JB6/AP-1 cell line, the Luciferase Assay system from Promega was followed according to manufacturer's instructions. Cells were seeded into 24-well plates at a density of 6 \times 10⁴ cells/well and exposed to either 50 $\mu\text{g}/\text{ml}$, 150 $\mu\text{g}/\text{ml}$ or 250 $\mu\text{g}/\text{ml}$ of ITO particles for 24 h. Tumor promoting agent (TPA) was used as a positive control.

2.10. Statistical analysis

For all analyses, the exposures were analyzed using a one-way layout to account for the unbalanced nature of the design, and thus allowing the inclusion of the positive control and the vehicle control in the analysis. Comparisons between sintered and unsintered exposures were evaluated using post hoc comparisons. Data for intracellular ROS were analyzed using SAS version 9.3 for Windows (SAS Institute, Cary NC). Using Proc Mixed, two-way analyses of variance with repeated measures on time were generated to assess interactions between variables. Pairwise comparisons between specific groups were extracted from these analyses using Fishers Least Significant Difference. For all other assays, one-way ANOVA was performed using Graphpad Prism version 6.0. Calculations for the percent damage of DNA in comet tails was performed with Perceptive Instruments Comet Assay IV. Statistical significance is shown when $p < 0.05$. Cellular assays were run in triplicate, with $n = 3$ for each.

3. Results

3.1. ITO particle characteristics and elemental analysis

Field emission scanning electron microscopy (FE-SEM) was used to determine the shape, structure, and size of ITO particles (Fig. 1A, B). Both SITO and UITO particles were $<5 \mu\text{m}$ in diameter. Elemental

analysis detected In, Sn, C and O as the only elements presents in the ITO particles (Fig. 1C).

3.2. Hydroxyl radical production from indium compounds

Acellular Fenton-like reactions showed that when reacted with H_2O_2 , UITO produced significantly more $\cdot\text{OH}$ radicals (as depicted by ESR peaks), when compared to both PBS and SITO (Fig. 2A). For cellular reactions, in both the RAW 264.7 and JB6/AP-1 cell lines (respectively), UITO once again produced significantly greater peaks in the ESR spectra, as compared to PBS and SITO exposed cells (Fig. 2B and C). SITO exposure produced a significant increase in $\cdot\text{OH}$ production when compared to the PBS vehicle control only in RAW 264.7 cells.

3.3. Decrease in cell viability is time- and dose-dependent

The fluorogenic peptide substrate GF-AFC was used to assess both RAW 264.7 and JB6/AP-1 cellular viability at the 4 h and 24 h timepoints. At 4 h, no significant changes in viability were detected between UITO and SITO exposed RAW 264.7 cells at matching doses. However, at both 150 $\mu\text{g}/\text{ml}$ and 250 $\mu\text{g}/\text{ml}$, SITO exposed cells did show significant decreases in viability when compared to the lowest dose of 50 $\mu\text{g}/\text{ml}$. This dose dependent decrease in viability was not, however, detected in UITO exposed cells. Additionally, only cells in the highest SITO exposure group demonstrated a significant decrease in viability compared to

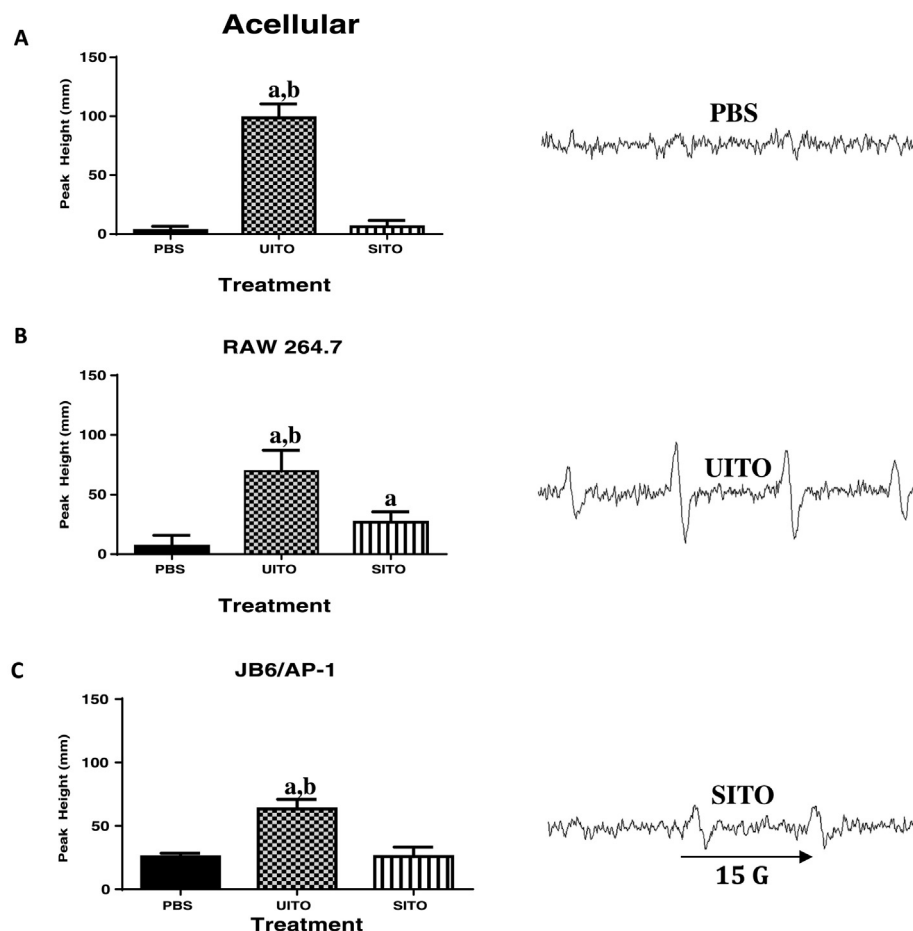


Fig. 2. Signal intensity (peak height) was used to measure the relative amount of $\cdot\text{OH}$ radicals generated by ESR. (A) Fenton-like reactions carried out in an acellular system using indium compounds and H_2O_2 show greater free radical production with UITO as compared to SITO and PBS. (B) Macrophage cells exposed to UITO produced significantly greater $\cdot\text{OH}$ radicals compared to those exposed to SITO and vehicle PBS controls. (C) Epidermal cells stably transfected with the AP-1 luciferase plasmid also showed greater $\cdot\text{OH}$ radical generation when exposed to UITO as compared to SITO. Representative ESR peaks are shown on right. ^a $P < 0.05$ vs. PBS; ^b $P < 0.05$ vs. SITO.

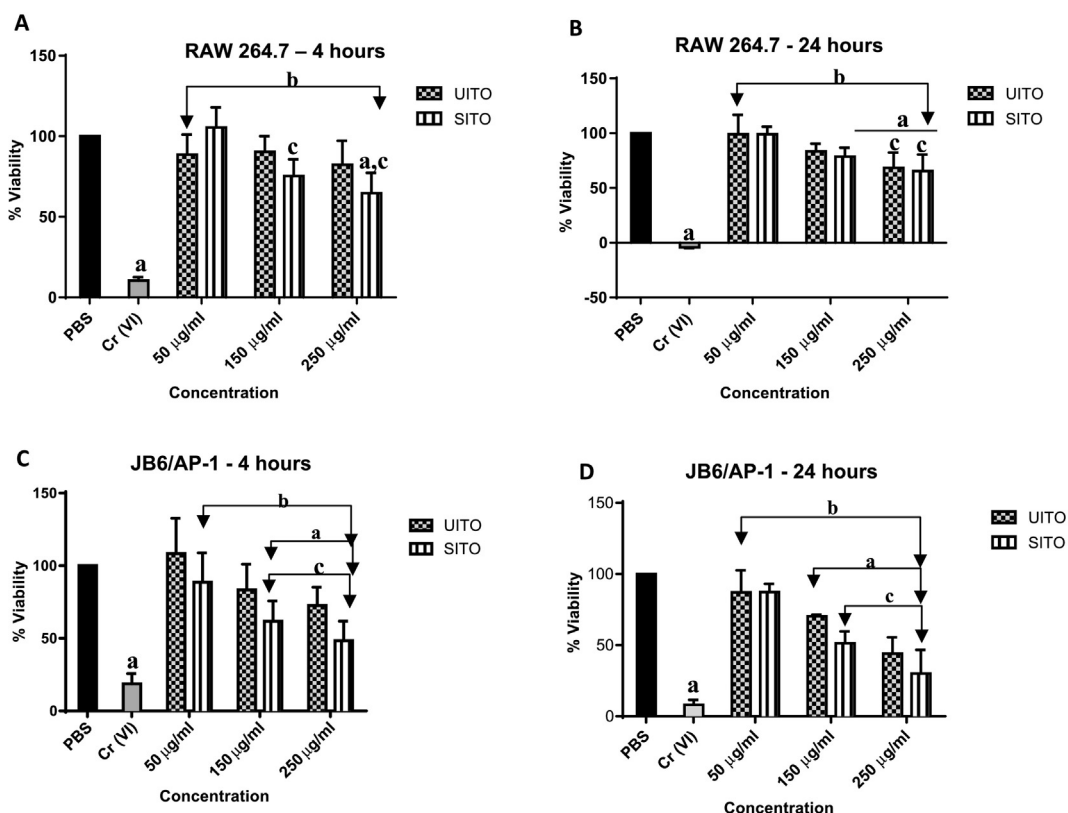


Fig. 3. Time and Dose Affect Cellular Viability. (A) At 4 h, RAW 264.7 cells exposed to SITO, but not UITO, exhibited a significant decrease in cell viability as concentration was increased. (B) At 24 h in RAW 264.7 cells, a 250 μ g/ml concentration of either UITO or SITO significantly decreased viability when compared to 50 μ g/ml. No significance was detected between UITO and SITO at matching concentrations. (C) JB6/AP-1 cells exposed to 150 μ g/ml or 250 μ g/ml UITO or SITO for 4 h showed significantly decreased viability compared to PBS controls. (D) In JB6/AP-1 UITO and SITO each caused concentration dependent decrease in viability at 24 h but no agent-dependent differences were observed at matching concentrations. Exposed vs. PBS: a P < 0.05; Exposed vs. Cr (VI): b P < 0.05; Compared to 50 μ g/ml within exposure group: c P < 0.05.

PBS controls (Fig. 3A). At 24 h, a significant decrease in RAW 264.7 viability was detected at 150 μ g/ml in SITO exposed cells when compared to PBS controls. At the highest dose of 250 μ g/ml, both UITO and SITO exposed cells had decreased viability when compared to both PBS controls and their respective 50 μ g/ml exposure groups (Fig. 3B). The viability of JB6/AP-1 cells appeared to be more sensitive to UITO and SITO exposure as compared to RAW 264.7 cells. For both UITO and SITO, 150 μ g/ml and 250 μ g/ml exposures each significantly decreased viability at the 4 h timepoint when compared to PBS controls. A dose-dependent decrease in viability was also observed (Fig. 3C). Significant decreases in the viability JB6/AP-1 cells was seen after exposure to 150 μ g/ml or 250 μ g/ml of either UITO or SITO (Fig. 3D). Hexavalent chromium [Cr (VI)] was used as a positive control for all experiments.

3.4. LDH release is time, treatment and dose dependent

Release of LDH from the cellular membrane into culture media was used to assess cell damage. At the 4 h timepoint, no significant difference was detected between vehicle controls and UITO and SITO exposed RAW 264.7 cells, regardless of dose (Fig. 4A). By 24 h, cells exposed to SITO exhibited significantly greater LDH release compared to those exposed to UITO at matching doses. In addition, compared to the lowest dose of 50 μ g/ml, LDH release significantly increased as dose was increased within exposure groups (Fig. 4B). LDH release in JB6/AP-1 cells at the 4 h timepoint was comparable to that of the RAW 264.7 cells, with no significant changes being detected between and within exposure groups (Fig. 4C). At 24 h, cell membrane damage in JB6/AP-1 cells was significantly greater in cells exposed to higher concentrations of UITO and SITO than at the 50 μ g/ml exposure. In addition, LDH release

was significantly greater in SITO than in UITO exposed cells at the 150 μ g/ml concentration (Fig. 4D).

3.5. DNA damage in comet tail increases with dose

The alkaline comet assay did not reveal any significant percentage of DNA in comet tails of RAW 264.7 exposed cells at the 3 h timepoint (data not shown). At 24 h, damage to the nuclear DNA of cells exposed to either UITO or SITO was significantly greater than PBS controls. Imaging revealed a heterogeneous response, with the majority of cells producing comet tails (Fig. 5A–E). The percentage of DNA found in comet tails was not significantly affected by the concentration of SITO exposure (Fig. 5F). However, in cells exposed to UITO, nuclear DNA damage was significantly greater in the 250 μ g/ml than in the 50 μ g/ml exposure (Fig. 5G).

3.6. Intracellular ROS generation increases with time

Dichloro-dihydro-fluorescein diacetate (DCFH-DA) was used to measure the intracellular production of ROS in cells over the course of time. Between 4 and 8 h, intracellular ROS generation in RAW 264.7 cells was significantly higher in cells exposed to Cr (VI) when compared to all other exposures. In addition, only at 8 h was any significant difference observed in intracellular ROS generation when comparing UITO and SITO exposed cells at 250 μ g/ml, with UITO causing greater ROS release (Fig. 6A). JB6/AP-1 cells responded to UITO and SITO exposure in the same manner as RAW 264.7 cells, with the only significant difference occurring at the highest dose at the 8 h timepoint, again with UITO generating greater ROS (Fig. 6B).

3.7. AP-1 pathway not activated in jb6 transfected cells

Compared to tumor promoting agent (TPA), exposing JB6 cells to UITO or SITO did not appear to activate the AP-1 pathway, which is involved in cellular proliferation, transformation and death (Fig. 7).

4. Discussion

Increased indium production and usage worldwide means that more workers are potentially being exposed in occupational settings. In 2014, the United States imported 123 metric tons of indium powders and unwrought indium metal, a 26% increase from 2013. In particular, ITO accounts for more than half of the global indium consumption (Tolcin, 2016). As the indium industry continues to grow, a better understanding of the toxicities associated with ITO exposure is warranted. Previous UITO and SITO comparative toxicity studies evaluated the cytotoxicity using samples which potentially contained traces of MWF, as often occurs in workplace settings (Badding et al., 2014). The traces of MWF may have influence cytotoxicity. The current study evaluates the cytotoxicity of UITO and SITO which have never been in contact with MWF.

The inhalation of indium in the occupational setting has been linked to pulmonary fibrosis which is characterized by scar formation in the lung tissue (Homma et al., 2003). ROS may play an etiologic role in idiopathic pulmonary fibrosis (Bocchino et al., 2010). Both acellular Fenton-like reactions and use of RAW 264.7 and the JB6/AP-1 cell lines yielded greater production of the •OH radical with UITO as compared

to SITO. Although UITO produced more •OH as measured by ESR, UITO was less cytotoxic than SITO as measured by LDH release. This suggests that •OH radical was not the major cause of cytotoxicity.

The atmosphere under which powders are sintered serve to protect formed compacts from oxidation and to reduce residual surface oxides. Processes such as sanding, cutting, and grinding can also impact occupational exposures. Other parameters such as time, temperature, powder composition and density of the powder compact are also important governing factors, thus causing changes in the material properties (Hoganas, 2013; Sharma and Madou, 2012). Because we were not given the specifics of sintering conditions from the indium collection site, it is hard to pinpoint what contributed to the decreased generation of •OH radicals in SITO as opposed to UITO. Nonetheless, our results are in line with the Kusrini laboratory, which also found that the process of sintering led to decreased free radical generation when measured with ESR, although they used bovine hydroxyapatite and not indium compounds (Kusrini and Sontang, 2012). On the contrary, Lison et al. has reported on ROS production by SITO in the presence of H₂O₂, which was not observed in our acellular system. This can perhaps be attributed to their higher concentrations of indium (36 mg/ml) and H₂O₂ (80 mM) used by Lison (Lison et al., 2009). With ITO, it is believed that free radical generation most likely occurs at reactive sites caused by the introduction of Sn into the crystal structure where there is high electron density (Fan and Goodenough, 2008a). The presence of indium salts on compound surfaces, regardless of sintering, also plays a role in their ability to generate ROS, as the dissolution of indium from ventilation dust

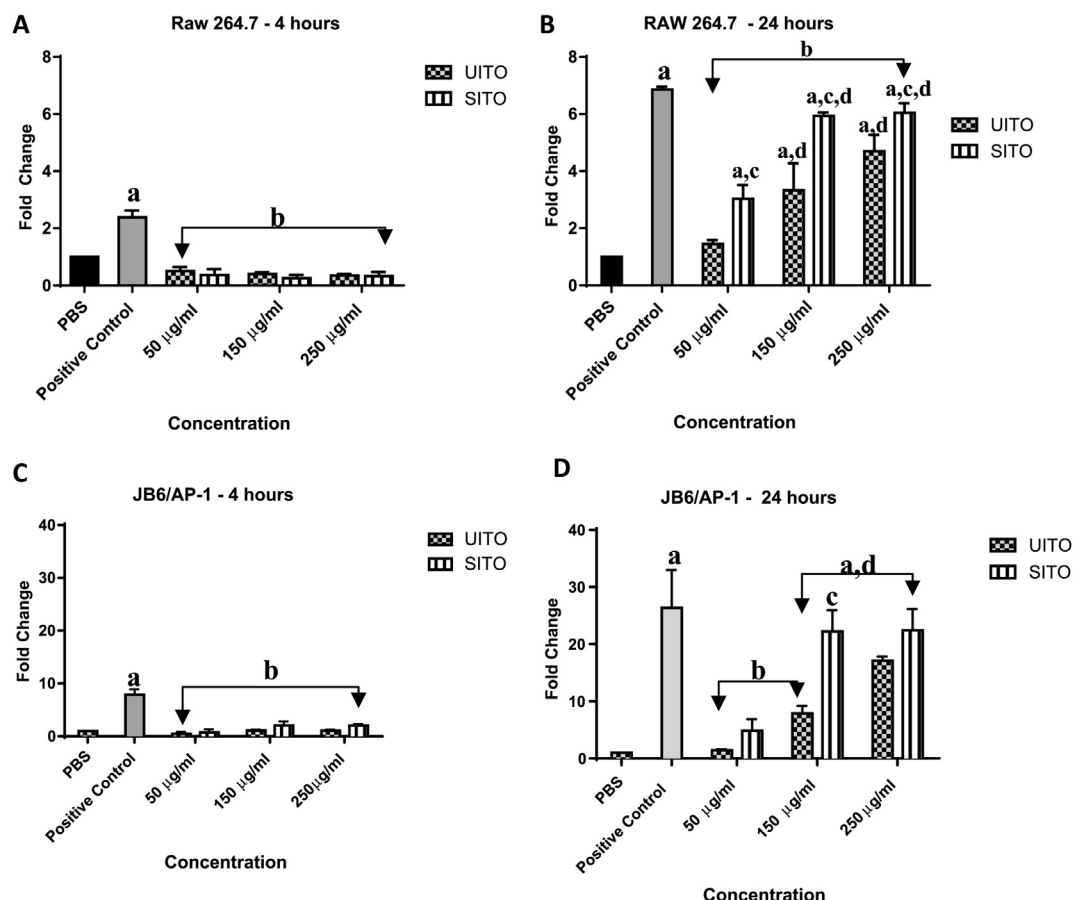


Fig. 4. LDH release is time, treatment, and dose dependent. (A) No significant difference was detected between LDH release from RAW 264.7 exposed to either UITO or SITO when compared to PBS at the 4 h timepoint. (B) At 24 h, UITO and SITO each produced a significant concentration-dependent increase in LDH release from RAW 264.7 cells. In addition, LDH release was significantly greater in SITO- compared to UITO-exposed cells at matching concentrations. (C) No significant difference was detected between cells exposed to either UITO or SITO when compared to PBS at the 4 h timepoint. (D) At 24 h, UITO and SITO each caused significantly greater damage to the cell membrane at higher concentrations when compared to 50 µg/ml. In addition, at matching concentrations a significant difference between UITO and SITO exposed cells was only detected at the 150 µg/ml concentration. Exposed vs. PBS ^aP < 0.05; Exposed vs. Positive Control ^bP < 0.05; SITO vs. UITO at matched concentrations ^cP < 0.05; Compared to 50 µg/ml within exposure group ^dP < 0.05.

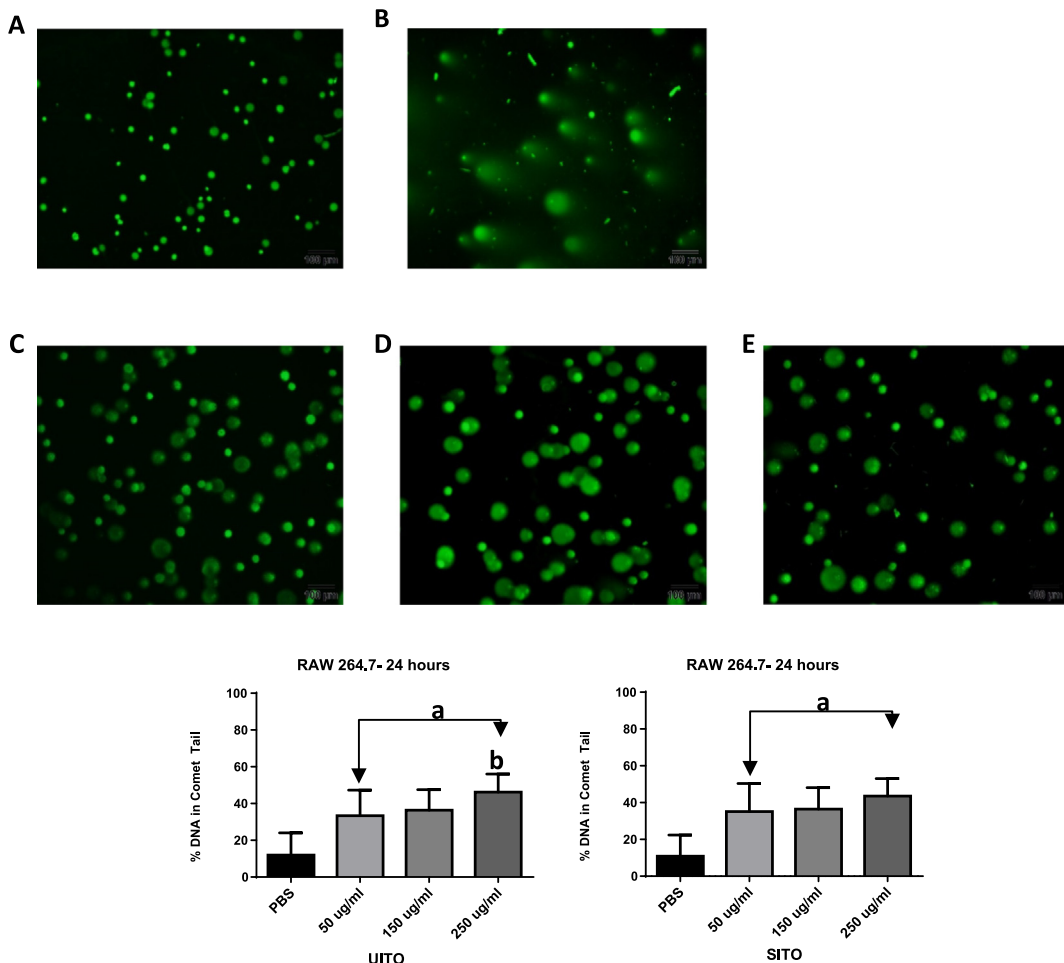


Fig. 5. DNA damage present in comet tails. The above micrographs are representative of RAW 264.7 cells were exposed to either (A) PBS; (B) 1 mM Cr (VI); (C) 50 µg/ml; (D) 150 µg/ml or (E) 250 µg/ml UITO or SITO for 24 h (UITO pictured). As dose increased, percent damage in the DNA comet tail was significantly increased when compared to PBS controls (F, G). Exposed vs. PBS ^aP < 0.05; Compared to 50 µg/ml ^bP < 0.05.

and reclaim byproduct in previous work generated significantly greater amounts of •OH when compared to both UITO and SITO (Badding et al., 2014).

The viability of both the RAW 264.7 macrophage and JB6/AP-1 epithelial cells were dependent on two factors, time, and dose. It has been suggested that the decrease in viability as seen with macrophage cells may be due to phagocytosis of the compounds in which ITO overwhelms the cells, inhibiting their capacity to function, and ultimately leading to death as a result of toxicity from engulfment of particles (Badding et al., 2014; Li et al., 2002). Compared to macrophage cells, the decrease in cellular viability was more apparent in the epithelial cells at both timepoints. Sintering did not play a role in the decreased viability, as UITO and SITO exposed cells did not exhibit significant differences in viability at matching concentrations.

In the workplace, reduced integrity or a barrier dysfunction of the skin can lead to increased dermal absorption of chemicals allowing for the entrance of larger molecules (Anderson and Meade, 2014). There is some evidence on the ability of UITO to stimulate an immune response in mice upon dermal exposure (Brock et al., 2014). In addition, Tinkle et al. have shown that particles as large as 1 µm in size can penetrate the intact epidermis (Tinkle et al., 2003). JB6 cells lack certain properties found in intact skin such as the stratum corneum barrier, and thus the interaction of keratinocytes with other cells (Jain et al., 1992). This lack of an intact barrier, along with the fact that all ITO used in this study were <5 µm in diameter could be contributing factors to the pronounced differences noted in decreased viability with JB6/AP-1 cells. Others studies have also reported on increased susceptibility of

epithelial cells to particle-induced death when compared to macrophages (Diabate et al., 2002; Xia et al., 2008).

The ability of ITO to generate ROS at the intracellular level was also studied. Interestingly, in both RAW 264.7 and JB6/AP-1 cells, intracellular ROS production was inversely related to the dose of both UITO and SITO, most likely a direct reflection of the decreased number of viable RAW 264.7 and JB6/AP-1 cells observed at higher concentrations.

Damage to the cellular membrane, as measured by LDH release, also showed vast differences between the RAW 264.7 and JB6/AP-1 cells. While the potential for particles to breach the epidermal barrier may have also contributed to greater membrane damage seen with epithelial cells, both cell lines demonstrated greater LDH release with SITO as opposed to UITO. Interestingly, Lison et al. also assessed the ability of ITO particles to induce LDH release but used rat lung epithelial cells (Lison et al., 2009). Even with their highest dose of 200 µg/ml, no effects were noticed at the 24 h timepoint. Perhaps the origin of the cells (pulmonary epithelial vs. epidermal epithelial) and/or the media used during exposure, particularly the presence of serum (which could influence particle dispersion) play a role in observed cytotoxicity. In our study it is clear that the process of sintering appears to generate a more potent product which induces cellular membrane damage in vitro.

Finally, the genotoxic and potential carcinogenic properties of ITO were also studied. Used to detect low levels of DNA damage in various cell types, the comet assay demonstrated that at 24 h, all three doses of UITO and SITO caused significantly greater damage to the nuclear DNA of RAW 264.7 cells when compared to PBS controls. However, comet tail increased with dose in UITO but not SITO exposed cells at

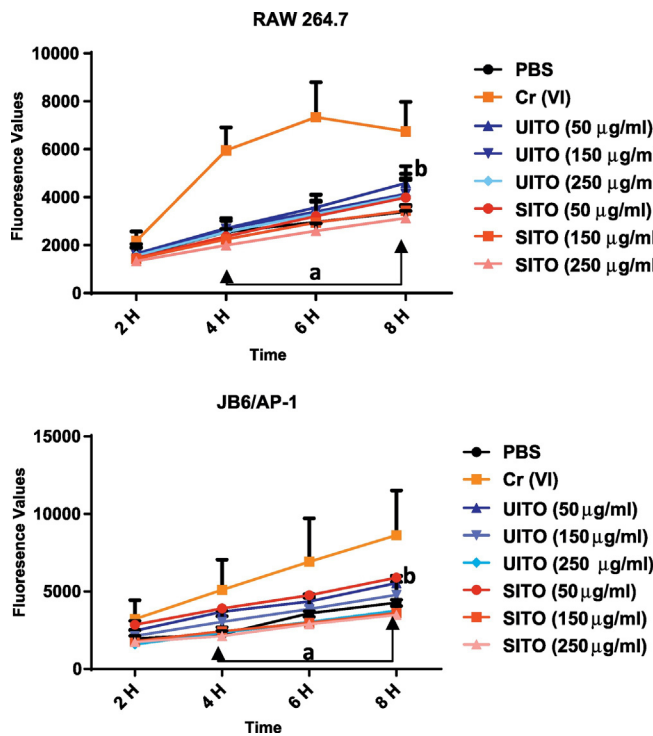


Fig. 6. Intracellular ROS generation increases with time. (A) Intracellular ROS generation in RAW 264.7 cells was significantly higher in cells exposed to Cr (VI) when compared to other exposures. Only at 8 h was any significant difference observed in intracellular ROS generation when comparing UITO and SITO exposed cells at the highest matching doses. (B) Cr (VI) caused greater intracellular ROS generation in JB6/AP-1 cells than other exposures. At 8 h a significant difference was observed in intracellular ROS generation when comparing UITO and SITO exposed cells at the highest matching doses. Treatment vs. Cr (VI): ^aP < 0.05; SITO vs. UITO (250 µg/ml): ^bP < 0.05.

24 h. This is in agreement with work done with ITO compounds containing trace endotoxin as a result of being in contact with MWF (Badding et al., 2014), suggesting that the MWF and endotoxin do not play an additional role in observed genotoxicities; the genotoxicity appears to be attributable to ITO.

Carcinogenesis is a multistage process which involves initiation, promotion, and progression (Pitot, 1993). The JB6 cells (P⁺; promotion sensitive) used in this study were stably transfected with the AP-1 luciferase plasmid. The transcription factor AP-1 plays a critical role in tumor promotion and progression, thus allowing for a better understanding of the tumor promoting potential of ITO compounds. In our study, when compared to the vehicle PBS control, ITO did not activate

the AP-1 pathway. Research on the carcinogenic properties of ITO compounds is mixed. Repeated inhalation studies in rats, but not in mice, to ITO aerosols resulted in bronchiolo-alveolar carcinomas and adenomas, though it remains unclear why rats were more susceptible (Nagano et al., 2011).

The results of our study, which utilized UITO and SITO which had not been in contact with MWF, are similar to the in vitro findings from ITO compounds that were in contact with MWF and endotoxin (Badding et al., 2014). Our study demonstrates that both UITO and SITO can cause •OH radical formation, cell membrane damage, and genotoxicity and cell death in vitro. While SITO had the greatest effect on cellular viability and LDH release, the toxicities observed with UITO were greater when looking at free radical generation and nuclear DNA damage, suggesting differences in cellular toxicity pathways and signaling mechanisms associated with different types of ITO exposure. It has been suggested that free radicals are likely generated at reactive sites as a result of the introduction of tin (Sn) in the overall compound structure, where electron density is high (Fan and Goodenough, 2008b).

Badding et al. has reported that the cytotoxic effects of SITO can in part be due to the activation of the NLRP3 inflammasome, known to induce the pro-inflammatory cytokine IL-1 β , thus causing subsequent cell death (Badding et al., 2015). Solubilization by macrophages in vitro of ITO compounds via the phagolysosomal acidification pathway, resulting in cell death and release of indium ions has also been shown (Gwinn et al., 2013). Though much work has been done in recent years studying the effects of ITO toxicity (Lison et al., 2009; Badding et al., 2015, 2016, 2014; Brock et al., 2014), the amount of conflicting data in relation to UITO- and SITO-mediated responses makes it apparent that the pathogenesis of ITO-mediated disease warrants further research.

Funding

This work was supported by intramural National Occupational Research Agenda (NORA) funding from NIOSH.

Conflict of interest

The authors have no conflicts of interest to report.

Disclaimer

The findings and conclusions in this report are those of the authors and do not necessarily represent the views of the National Institute for Occupational Safety and Health.

Acknowledgements

The authors would like to thank the laboratory of Dr. Min Ding (NIOSH, Morgantown, WV) for the generous donation of the JB6 cells stably transfected with the AP-1 luciferase plasmid. We would also like to thank Linda Bowman (NIOSH, Morgantown, WV) for her help and expertise in working with the JB6/AP-1 cell line.

References

- Anderson, S.E., Meade, B.J., 2014. Potential health effects associated with dermal exposure to occupational chemicals. *Environ. Health Insights* 8 (Suppl. 1), 51–62.
- Badding, M.A., et al., 2014. Cytotoxicity and characterization of particles collected from an indium-tin oxide production facility. *J. Toxicol. Environ. Health A* 77 (20), 1193–1209.
- Badding, M.A., et al., 2015. Sintered indium-tin oxide particles induce pro-inflammatory responses in vitro, in part through inflammasome activation. *PLoS One* 10 (4), e0124368.
- Badding, M.A., et al., 2016. Pulmonary toxicity of indium-tin oxide production facility particles in rats. *J. Appl. Toxicol.* 36 (4), 618–626.
- Biswas, R., Bunderson-Schelman, M., Holian, A., 2011. Potential role of the inflammasome-derived inflammatory cytokines in pulmonary fibrosis. *Pulm. Med.* 2011, 105707.
- Bocchino, M., et al., 2010. Reactive oxygen species are required for maintenance and differentiation of primary lung fibroblasts in idiopathic pulmonary fibrosis. *PLoS One* 5 (11), e14003.

Fig. 7. ITO does not activate the AP-1 pathway. Compared to PBS, indium tin-oxide (both sintered and unsintered) did not significantly activate the AP-1 pathway in JB6 cells. Exposed vs. PBS: ^aP < 0.05.

Brock, K., et al., 2014. Immune stimulation following dermal exposure to unsintered indium tin oxide. *J. Immunotoxicol.* 11 (3), 268–272.

Cummings, K.J., et al., 2012. Indium lung disease. *Chest* 141 (6), 1512–1521.

Diabate, S., et al., 2002. In vitro effects of incinerator fly ash on pulmonary macrophages and epithelial cells. *Int. J. Hyg. Environ. Health* 204 (5–6), 323–326.

Fan, J.C.C., Goodenough, J.B., 2008a. X-ray photoemission spectroscopy studies of Sn-doped indium-oxide films. *J. Appl. Phys.* 48, 3524–3531.

Fan, J.C., Goodenough, J.B., 2008b. X-Ray photoemission spectroscopy studies of Sn-doped indium-oxide films. *J. Appl. Phys.* 48, 3524–3531.

Gilbert, Y., Veillette, M., Duchaine, C., 2010. Metalworking fluids biodiversity characterization. *J. Appl. Microbiol.* 108 (2), 437–449.

Gwinn, W.M., et al., 2013. Macrophage solubilization and cytotoxicity of indium-containing particles in vitro. *Toxicol. Sci.* 135 (2), 414–424.

Hines, C.J., et al., 2013. Use of and occupational exposure to indium in the United States. *J. Occup. Environ. Hyg.* 10 (12), 723–733.

Hoganas, 2013. In: AB, H. (Ed.), *Production of Sintered Components-Hoganas Handbook of Sintered Components* (Sweden).

Homma, T., et al., 2003. Interstitial pneumonia developed in a worker dealing with particles containing indium-tin oxide. *J. Occup. Health* 45 (3), 137–139.

Jain, P.T., et al., 1992. Studies of skin toxicity in vitro: dose-response studies on JB6 cells. *Toxicol. Pathol.* 20 (3 Pt 1), 394–404.

Jomova, K., Valko, M., 2011. Advances in metal-induced oxidative stress and human disease. *Toxicology* 283 (2–3), 65–87.

Kang, M.I., et al., 2009. A selective small-molecule nuclear factor- κ B inhibitor from a high-throughput cell-based assay for "activator protein-1 hits". *Mol. Cancer Ther.* 8 (3), 571–581.

Kusrimi, E., Sontang, M., 2012. Characterization of x-ray diffraction and electron spin resonance: effects of sintering time and temperature on bovine hydroxyapatite. *Radiat. Phys. Chem.* 81 (2), 118–125.

Leonard, S.S., Harris, G.K., Shi, X., 2004. Metal-induced oxidative stress and signal transduction. *Free Radic. Biol. Med.* 37 (12), 1921–1942.

Li, N., et al., 2002. Comparison of the pro-oxidative and proinflammatory effects of organic diesel exhaust particle chemicals in bronchial epithelial cells and macrophages. *J. Immunol.* 169 (8), 4531–4541.

Lison, D., et al., 2009. Sintered indium-tin-oxide (ITO) particles: a new pneumotoxic entity. *Toxicol. Sci.* 108 (2), 472–481.

Nagano, K., et al., 2011. Inhalation carcinogenicity and chronic toxicity of indium-tin oxide in rats and mice. *J. Occup. Health* 53 (3), 175–187.

Nakano, M., et al., 2015. Pulmonary effects in workers exposed to indium metal: a cross-sectional study. *J. Occup. Health* 57 (4), 346–352.

Nakano, M., et al., 2016. An advanced case of indium lung disease with progressive emphysema. *J. Occup. Health* 5, 477–481.

NIOSH, 2012. Hazard Evaluation and Technical Assistance Report: An Evaluation of Preventive Measures at an Indium-Tin Oxide Production Facility. Department of Health and Human Services, Public Health Service, Centers for Disease Control and Prevention, Morgantown, WV.

Pitot, H.C., 1993. The molecular biology of carcinogenesis. *Cancer* 72 (3 Suppl), 962–970.

Ruocco, K.M., et al., 2007. A high-throughput cell-based assay to identify specific inhibitors of transcription factor AP-1. *J. Biomol. Screen.* 12 (1), 133–139.

Sharma, S., Madou, M., 2012. A new approach to gas sensing with nanotechnology. *Philos. Trans. A Math. Phys. Eng. Sci.* 370 (1967), 2448–2473.

Tinkle, S.S., et al., 2003. Skin as a route of exposure and sensitization in chronic beryllium disease. *Environ. Health Perspect.* 111 (9), 1202–1208.

Tolcin, A.C., 2016. 2014 Minerals Yearbook: Indium (Advance Release). United States Geological Survey.

U.S.G.A.O, 2005. Report to Congressional Requesters: Chemical Regulation Options Exist to Improve EPA's Ability to Assess Health Risks and Manage Its Chemical Review Program.

Xia, T., et al., 2008. Cationic polystyrene nanosphere toxicity depends on cell-specific endocytic and mitochondrial injury pathways. *ACS Nano* 2 (1), 85–96.